Journal of Analytical and Applied Pyrolysis 99 (2013) 170–177

Contents lists available at SciVerse ScienceDirect

Journal of Analytical and Applied Pyrolysis

journal homepage: www.elsevier.com/locate/jaap

Pyrolysis of orange waste: A thermo-kinetic study

M.A. Lopez-Velazquez[a], V. Santes[a], J. Balmaseda[b], E. Torres-Garcia[c,*]

[a] Depto. de Biociencias e Ingeniería, CIIEMAD, Instituto Politécnico Nacional, Calle 30 de junio de 1520, Col. Barrio la Laguna Ticomán, Gustavo A. Madero, México, D.F. 07340, Mexico
[b] Departamento de polímeros, Instituto de Investigaciones en Materiales, Universidad Nacional Autónoma de México, México, D.F. C.P. 04510, Mexico
[c] Instituto Mexicano del Petróleo, Eje Central # 152, México, D.F. 07730, Mexico

ARTICLE INFO

Article history:
Received 29 May 2012
Accepted 30 September 2012
Available online 8 October 2012

Keywords:
Pyrolysis of orange waste
Bio-energetic
Ligno-cellulosic
Kinetics
TGA–FTIR

ABSTRACT

Thermal and kinetic decomposition of orange waste have been investigated by simultaneous TGA–DSC and TGA–FTIR analysis techniques under nitrogen atmosphere. Thermal profile degradation can be interpreted as the resultant of multiple, parallel and simultaneous reactions, related to: (i) dehydration process for temperatures ≤120 °C; (ii) pyrolytic cracking, from 125 to 450 °C, stage where the ligno-cellulosic components are degraded reaching a maximum the evolved gaseous products and delivery energy; and (iii) to latest stage of lignin degradation, at temperatures ≥450 °C. The volatile compounds evolved from 50 to 600 °C were mainly: H_2O, CO_2 and CO, besides of a mixture organic product composed by: carboxylic acids, aldehydes or ketones (C═O), alkanes (C—C), ethers (C—O—C), alcohols (C—O—H), phenolic compounds (C—O) and aliphatic and/or unsaturated aromatic compounds (C═C). Kinetic parameters were calculated by two kinds of model-free kinetics algorithms, Friedman (*F*) and Kissinger–Akahira–Sunose (KAS) methods at different heating rates (5, 10 and 15 °C min^{-1}). The results in terms of activation energy show the complex $E_a(\alpha)$ on α dependence, which evidences an multi-step kinetic processes during the pyrolytic cracking of the orange waste.

1. Introduction

Increasing environmental concerns about excessive net carbon dioxide emissions, the steadily decrease of easily accessible fossil fuels, and the rising demand for a secure supply of fuel, chemical, and energy have increased the interest in renewable and sustainable sources [1,2].

Citrus fruits crops are the most abundant in the world, producing over 120 million tons of oranges, lemons, grapefruits and mandarins [3]. In Mexico, orange farming is both an important industry and also a paramount source of financial incomes in zones of high production. Only in 2010, the orange production reached about 4 million tons, from which the 40% (about 1.6 million tons of the total produced), are converted into wet solid residues, corresponding approximately to 800,000 tons of dry residue [4]. In this context, the disposal of any waste is a worry in the area of environmental protection and sustainability. Therefore, citrus wastes, which are generated during industrial process to produce juices, are seen as a problematic but unavoidable by-waste. As a residual byproduct of the juices industry, these citrus wastes do not find commercial applications and are largely disposed of in open dumps. Among the most traditional option for disposal is its application to land, thus providing a source of slow-release nutrients and microelements, as underutilized cattle feed, or in the cosmetic industry. In general, the citrus fruit residues represent an abundant, inexpensive and readily available source of renewable biomass and their utilization are attracting increased interests around all over the world. This is because that the ligno-cellulosic waste, represent a suitable sustainable source for production of conventional and new chemicals and fuels [5,6]. Therefore, developments of new methods to treat citrus waste are urgently required.

Recently, many researchers have carried out characterization studies of ligno-cellulosic biomass such as pyrolysis, thermolysis, gasification, and combustion in order to design efficient and environmentally sustainable processes. Biomass properties can significantly influence both heat transfer and reaction rates, such that the optimal operating conditions are highly variable [7–9]. Pyrolysis is one of the most employed methods to convert biomass and organic residues into diverse products [4,5]. Its application may essentially diversify the energy-supply in many situations, leading to a more secure and sustainable global energy-supply chain. Therefore, research on the pyrolysis process of a specific ligno-cellulosic waste, would be beneficial for a better understanding of the pyrolytic-cracking mechanism and to improve its transformation and application as bio-fuels, chemical products and bio-materials [10–13]. So, among the many reasons for quantifying the rate of a chemical reaction, the thermo-kinetic behavior of the biomass is of high importance during the degradation of its main components, which allow control the reaction rate as a function of temperature, pressure, and composition. Hence, the information

* Corresponding author. Tel.: +52 55 9175 8430; fax: +52 55 9175 8429.
E-mail addresses: etorresg@imp.mx, eneliot@yahoo.es (E. Torres-Garcia).

0165-2370/$ – see front matter © 2012 Elsevier B.V. All rights reserved.
http://dx.doi.org/10.1016/j.jaap.2012.09.016

about biomass pyrolysis kinetics is necessary to accurately predict reactions behavior, as well as to optimize and control the process of conversion toward products during the pyrolytic degradation.

Regardless of the numerous studies on biomass pyrolysis kinetics, only a few studies have been focused on the processes taking place during the pyrolysis of orange waste [14,15]. However, an analysis of the kinetic data and detailed research on the pyrolysis gaseous products at different reaction temperatures has not been reported. The situation is particularly complicated, because the thermal degradation of the orange waste is a complex process, where a number of consecutive and parallel reactions are involved. In correspondence, the aim of this work is to provide a detailed analysis of the thermal degradation kinetics, along with the evolution of the volatile products for each step of the pyrolytic process.

2. Materials and methods

2.1. Samples preparation

The orange waste (pulp) used in this study as ligno-cellulosic biomass was supplied by a juice production industry of the Alamo municipality, Veracruz State in Mexico. Orange waste sample was submitted to several treatments before analysis. Firstly, it was dried at room temperature during eight days. Secondly, it was dried in a furnace at 110 °C in air static for 24 h. The moisture content after these two steps was 7%, which was determined at 100 °C via TGA. Finally, the orange waste was ground to size <1 mm using a Hobar cutting mill model FT100. The resulting samples were sieved on a Retsch sieve shaker model AS 400 for 10 min and fractions between 300–180, 180–150 and <150 μm, were collected and stored in sealed polyethylene bags.

2.2. Samples characterization

To determine the chemical characteristics of orange waste, elemental and proximate analyses were carried out, and the main information is summarized in Tables 1 and 2. Proximate analyses of the samples were performed based on ASTM methods E871, E872-82 and D1102-84. Meanwhile, the elemental analysis was performed in a CHN/O Vario EL analyzer using the ASTM D5291 method. The sulfur content was determined in a HORIBA SLFA-1800 equipment by ASTM D4294 method. Ash content was obtained following the ASTM D482 method in Limberth muffle. Chlorine content was measured in a Mitsubishi X-10 by using the EPA 953 method. The oxygen content was obtained by a mass balance among C, H and N.

Table 1
Ultimate analysis of orange waste.

Elemental composition (dry basis)	wt.%
Carbon	47.0
Hydrogen	6.9
Nitrogen	1.3
Oxygen[a]	44.71
Sulfur	0.09
Chloride	0.001

[a] The oxygen content is calculated by difference.

Table 2
Proximate analysis of orange waste.

Components	wt%
Volatile matter	74.6
Fixed carbon	16.68
Ash	3.02
Water	5.7

The FTIR spectra were employed to analyze the original orange waste. The samples were mixed with KBr powder and dried in an oven at 100 °C for 24 h. FTIR spectra were recorded in a Nicolet Nexus Spectrometer.

2.3. Thermal analysis (TGA–DSC)

Thermal degradation of orange waste samples was carried out in a simultaneous TGA–DSC (NEZTZSCH STA 409 PC). To mitigate the difference of heat and mass transfer, the sample mass was kept at ~5 mg. The samples were heated from room temperature up to 700 °C at a constant heating rate of 10 °C min^{-1}, using an ultra-dry nitrogen atmosphere and a flow rate of 100 mL min^{-1}.

2.4. TGA–FTIR simultaneous measurements

Evolved gas analysis of waste pyrolysis was carried out in NICOLET Protégé 460 FTIR spectrometer coupled to a TA Instrument's 2950 thermogravimetric analyzer. The transfer line and gas cell of the spectrometer were heated to 240 °C to avoid condensation or adsorption of semi-volatile products. Each IR spectrum was recorded every 5 s from 4000 to 500 cm^{-1}.

TGA experiments were performed at different heating rates of 5, 10, 15 °C min^{-1} and the DTG data collected at different heating rates were used to obtain information about the amount, magnitude and nature of the different processes and to estimate the apparent activation energy involved in each stage and its dependence on the degree of reaction extent α. The mass samples were about 10 mg in all cases and the sensitivity of the balance was 10^{-7} g.

3. Kinetic study

3.1. Model-free method

Model free kinetics is based on an isoconversional method where the activation energy is a function of the conversion degree of a chemical reaction. Applications of model-free methods are highly recommended by the Kinetics Committee of the International Confederation for Thermal Analysis and Calorimetry (ICTAC Kinetics Committee) [16]. To validate this recommendation, the ICTAC Kinetics Committee has conducted an extensive comparison study between different methods and found that the model-free and multi-heating rate methods are particularly successful in describing the multi-step kinetic processes.

In this work, we have combined two kinds of model-free-kinetics algorithms to predict the pyrolytic cracking kinetics of orange waste.

Both are based on Eq. (1):

$$\frac{d\alpha}{dt} = k(T)f(\alpha) = A\exp\left(-\frac{E_a}{RT}\right)f(\alpha) \quad (1)$$

where α is the degree of conversion, $f(\alpha)$ is the reaction model, T (K) is the absolute temperature, A (s^{-1}) is the pre-exponential factor, E_a (kJ/mol) is the activation energy, and R is the universal gas constant.

All isoconversional methods have their origin in the isoconversional principle which states that the reaction rate at constant extent of conversion is only a function of temperature [17].

$$\frac{d\ \ln(d\alpha/dt)_\alpha}{dT^{-1}} = -\frac{E_a}{R} \quad (2)$$

where α denotes the extent of reaction, t is time, T is absolute temperature, R is the gas constant and E_a is the activation energy as a function of the extent of degradation.

By rearranging and integrating Eq. (2), one can easily arrive at Eq. (3).

$$\ln\left(\frac{d\alpha}{dt}\right)_{\alpha} = \text{constant} - \frac{E_a}{RT} \tag{3}$$

which is the basis of the differential isoconversional method of Friedman [18]. The apparent activation energy can be obtained from the slope of the linear plot of $\ln(d\alpha/dt)_\alpha$ vs $1000/T$ for each value of conversion, α, where the slop equals E_a/R.

Another model-free-kinetics algorithms choice was the Kissinger–Akahira–Sunose (KAS) method [19], which simply consists of extending the Kissinger method [20]. The KAS method requires the temperature values $T_\alpha(\beta)$ at which an equivalent conversion degree of reaction occurs for various heating rates β ($\beta = dT/dt = \text{const}$). The equivalent transformation is either defined as the stage at which a fixed amount is transformed or as the stage at which a fixed fraction of the total amount is transformed.

Such that:

$$g(\alpha) = \int_0^{\alpha} \frac{d\alpha}{f(\alpha)} = \frac{A}{\beta}\int_{T_0}^{T_\alpha} e^{-E_a/RT}\,dT = \frac{AE_a}{R\beta}\cdot p\left(\frac{E_a}{RT}\right) \tag{4}$$

Since the integral p in Eq. (4) does not have an analytical solution it can be solved taking into account the following approximation on the p function [21]:

$$p\left(\frac{E_a}{RT}\right) \approx \frac{e^{-E_a/RT}}{(-E_a/RT)^2} \tag{5}$$

The logarithm of Eq. (4) gives:

$$\ln\left(\frac{\beta_j}{T_{jk}^2}\right) = \left[\ln\left(\frac{A(\alpha_k)\cdot R}{E_a(\alpha_k)}\right) - \ln\ g(\alpha_k)\right] - \frac{E_a(\alpha_k)}{RT_{jk}} \tag{6}$$

where the apparent activation energy $E_a(\alpha_k)$ and the pre-exponential factor $A(\alpha_k)$ are expressed for a given conversion degree α_k and the temperatures T_{jk} are the temperatures at which the conversion α_k is reached at a heating rate β_j. If $\alpha_k = \text{const}$ and reaction is independent of the heating rates, then $g(\alpha_k)$ is also constant for a given conversion degree and temperature. During a series of measurements the heating rates are $\beta = \beta_1, \ldots, \beta_j \ldots$. The apparent activation energy can be obtained from the slope of the linear plot of $\ln(\beta_j/T_{jk}^2)$ against $1000/T_{jk}$ for each value of conversion, α_k, where the slop equals $-E_a(\alpha_k)/R$.

The purpose of choosing those two kinds of models-free kinetics algorithms was to validate and to corroborate the consistence of our results through two different algorithms: the differential one of Friedman (F) and the integral one of Kissinger–Akahira–Sunoe (KAS).

4. Results and discussion

4.1. Characterization of the initial ligno-cellulosic biomass

FTIR spectrum of the dried orange waste is shown in Fig. 1. The spectrum analysis indicates the presence of characteristic bands corresponding to cellulose, as well as of lignin [9,22]. The most intense band in the high energy zone (3000–3600 cm^{-1}) is assigned to the existence of free and intermolecular bonded hydroxyl groups, related to a large amount of OH groups from carbohydrates and those of lignin, as well as to the symmetric and asymmetric stretching vibrations associated with H_2O molecules. The intense band at 1045 cm^{-1} corresponds to the link C—O—H or C—O—R (alcohols or esters), while the distinctive band at 2925 cm^{-1} is related to the presence of C—H stretching vibration together with bending vibrations around 1428 cm^{-1} of aliphatic chains (—CH_2— and —CH_3—) forming the basic structure of these ligno-cellulosic materials [23].

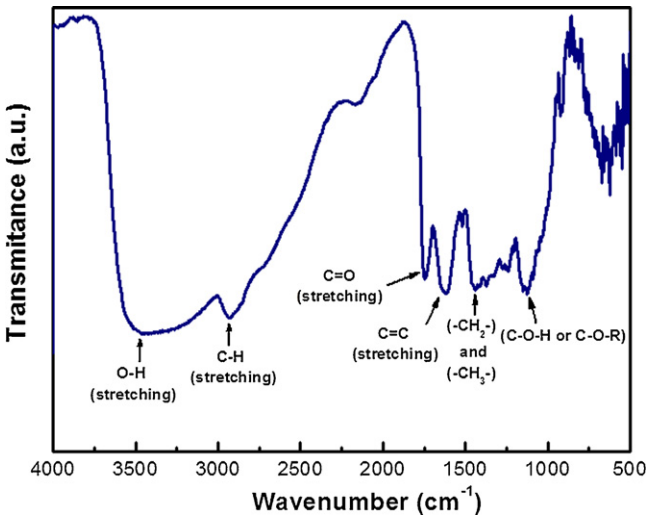

Fig. 1. FTIR spectrum of the dried orange waste sample.

The peak at 1736 cm^{-1} is attributable to carboxylic acid and/or carbonyl groups of esters. Finally, the band at 1620 cm^{-1} can be attributed to aliphatic and/or unsaturated aromatic compounds [24].

4.2. Thermal behavior

A typical thermal profile of the dried orange waste, obtained by simultaneous TGA–DSC in nitrogen, is shown in Fig. 2, which depicts the experimental TGA–DSC thermograms for an experiment performed at $\beta = 10\,^{\circ}C\,min^{-1}$. In general, the main thermal processes up to 700 °C, are related to the dehydration process and thermal degradation of the ligno-cellulosic biomass [25,26]. Orange waste is considered to be composed of various constituents (hemicelluloses, cellulose and lignin), which decompose at different temperature regions [8,9,27]. Initial mass loss of 7.5 mass%, for temperatures lower to 120 °C, is related to the release of weakly bonded water molecules (physically adsorbed water molecules), without excluding the simultaneous evolution of some organic volatile compounds. This explains the origin of the exothermic behavior at temperature below 100 °C (see DSC curve, Fig. 2).

After the dehydration process, several overlapped weight losses with identified maxims at 165 °C, 212 °C, 254 °C and 328 °C; as well as a prolonged weight loss from 380 to 550 °C are detected.

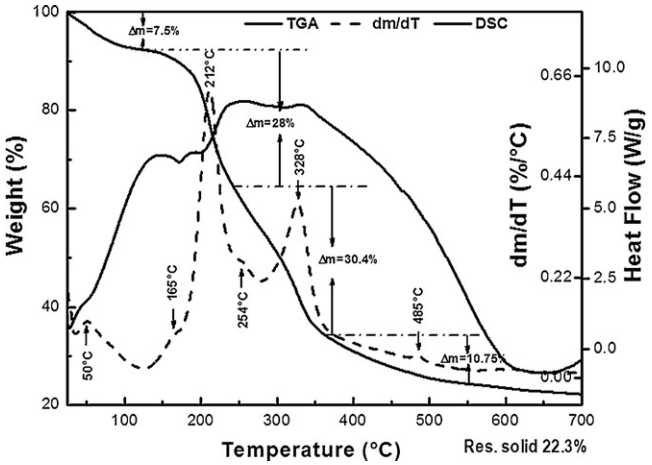

Fig. 2. Simultaneous TGA–DSC curves of the thermal decomposition of orange waste under flowing dry N_2 (100 mL min^{-1}) and heating rate of 10 °C min^{-1}.

Accordingly, the DSC curve shows several and overlapped exothermic processes around from 50 to 600 °C. The delivery energy, as well as the weight losses in this wide temperature interval can be related to biomass degradation, essentially, to its main components (hemicelluloses, cellulose and lignin) [8,9]. The first stage, from ~125 to 250 °C, associated to a 28% weight loss, is attributed essentially to the decomposition of hemicelluloses. Following, one contiguous and/or simultaneous process between 250 and 360 °C, with a 30.4% weight loss, is ascribed to the cellulose degradation. It should be noted that although these two stages are mainly characterized by the degradation of both hemicelluloses and cellulose, lignin simultaneous decomposition is also present at that temperature interval. Finally, a prolonged weight loss of ~11 mass %, in the 380–550 °C range, with a maximum at ~485 °C in the DTG curve, might be attributed to the last stage of degradation of lignin. That behavior has been previously reported by others [25,28].

In summary, during the pyrolytic process up to 700 °C, around 77 wt.% of the ligno-cellulosic biomass can be volatilized, with a 22% of residual materials, besides about ~7 wt.% of water.

4.3. Effect of particle size

The particle size effect is a very important experimental study to predict, optimize and control any thermal degradation process such as combustion, pyrolysis or gasification of biomass. The size of the ligno-cellulosic biomass particle is one of the parameters that can strongly affect the energy efficiency improvement, the completion time of the pyrolytic process and the nature of the reaction products (solids, liquid or gaseous).

In order to establish the influence of particles size on the cracking pyrolytic process, three different particle size fractions of orange waste (300–180, 180–150 and <150 μm) were studied. Fig. 3a and b, display both the weight loss rates (represented in their derivative form DTG) and the delivery energy through the DSC curves.

In all samples the major degradation and maximum devolatilization rate of the orange waste occurs between 120 and 400 °C. However, the heat released, as shown in the DSC curve, presents a wide interval with several overlapped exothermic peaks between 50 and 600 °C. These experimental evidences suggest that the particle sizes only have influence on the thermal behavior at the start and end of pyrolysis process, especially for the samples with particles size lower than <150 μm. This behavior can be rationalized in terms of the heat- and mass-transfer phenomena, which stems from the difference specific surface area among the particle sizes studied.

The biomass conversion into different products during the pyrolytic cracking process cannot be resolved based solely on a TGA–DSC study, these techniques by themselves do not provide specific information about of the nature of the chemical species evolved, and the assignment and interpretation of each thermal event is not obvious. Therefore, we focused our attention on a more detailed analysis of the possible specific chemical species, through its identification by in situ IR (FT-IR) and we used as a model the orange waste sample which particle size is in the 180–150 μm range.

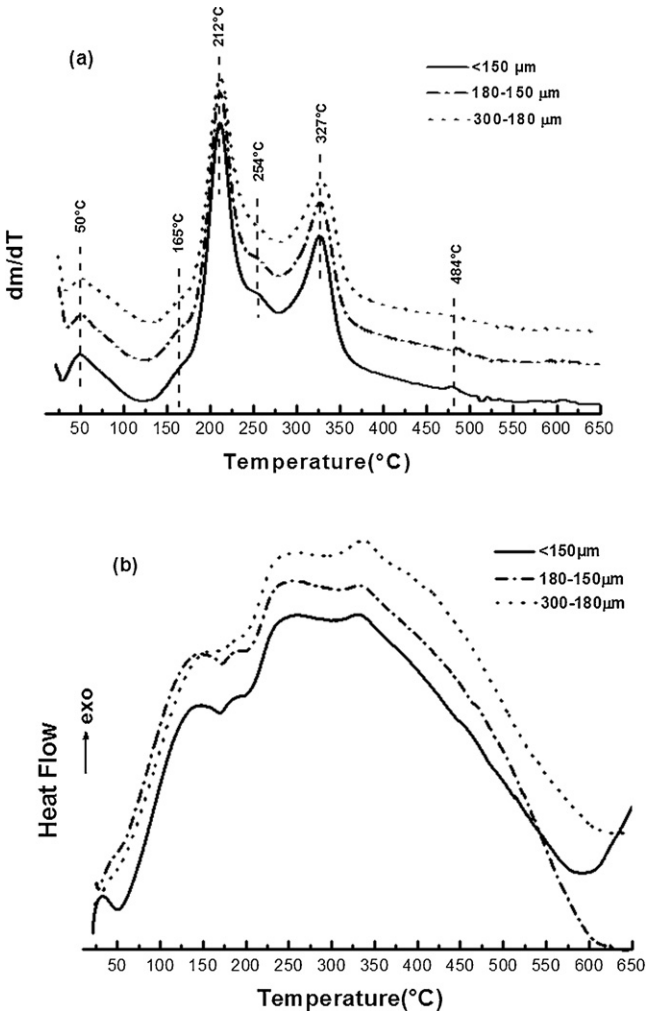

Fig. 3. Effect of particles size on DTG and DSC thermal profiles.

4.4. Evolved gas analysis (TGA–FTIR)

Simultaneous TGA–FTIR techniques were applied to obtain information of the reaction sequences and the most relevant gaseous products of decomposition between 50 and 600 °C. During the pyrolytic cracking process the gases released in the TG were

Table 3
The main functional groups identified by FTIR.

Wave number	Functional group
Broad band 3760–3580 cm^{-1}	Symmetric and asymmetric stretching vibrations associated with H_2O molecules
Bands about 3900–3700 cm^{-1}	Rota-vibrational band of water vapor
Doublet at 3327–2365 cm^{-1} and single peak at 670 cm^{-1}	CO_2 presence
Doublet on 2200–2000 cm^{-1}	CO presence
Peaks at 2937 and 2849 cm^{-1}	Symmetrical and asymmetrical C—H stretching vibrations of aliphatic —CH_3 and —CH_2— groups
Bands at 3014 cm^{-1}	Characteristic of CH_4
Peaks at 1480 and 1450 cm^{-1}	C—H bonds of hydrocarbons
Bands at 1100–1030 cm^{-1}	Alcohols C—O—H bond involving a saturated carbon
Peaks on 1800–1650 cm^{-1}	Assigned to C=O stretching vibrations of carboxylic acid and/or carbonyl
Peaks at 1240 and 1185 cm^{-1}	Assigned to C—O stretching vibrations of phenolic oxygen
1620–1580 cm^{-1} range	Attributed to C=C group of aliphatic and/or unsaturated aromatic compounds

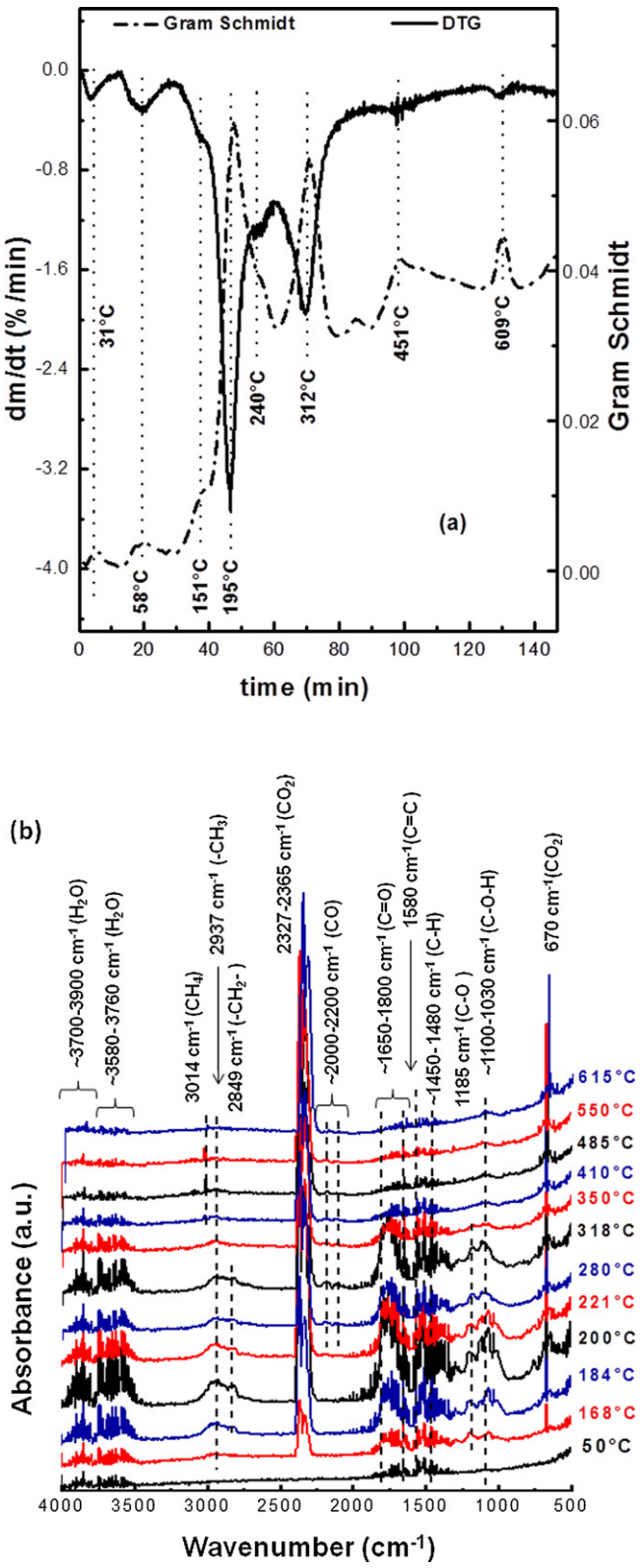

Fig. 4. (a) Changes in IR intensity (Gram Schmidt), and its relationships with *dm*/*dt* as a function of time. (b) Stacked plot of FTIR spectra of the evolved gases for orange waste during its degradation to different temperature intervals.

swept immediately to a gas cell, followed by FTIR analysis (see changes in IR intensity as a function of time, Fig. 4a). The IR spectra during all process are shown in Fig. 4b, where the temperature is referred to that in the TGA. Based on the analysis of FTIR spectra, the main functional groups identified are summarized in Table 3.

According to the FTIR study, the evolution of gaseous products, mainly H_2O, CO_2, CO and a mixture of organic products, increases with the pyrolysis temperature, reaching its maximum between 150 and 400 °C. Generally, peaks between ~3760 and 3580 cm^{-1} are assigned to the symmetric and asymmetric stretching vibrations of H_2O molecules. Meanwhile, the signals about 3700–3900 cm^{-1}, may correspond to a rota-vibrational band of water vapor [29].

The presence of CO_2 was identified by the doublet at 2365–3327 cm^{-1}, which is confirmed by a singlet at 670 cm^{-1}, while, the doublet of 2200–2000 cm^{-1}, is ascribed to CO. The peaks at 2937 and 2849 cm^{-1} were ascribed to symmetrical and asymmetrical C—H stretching bands of the aliphatic —CH_3 and —CH_2— groups [23]. An interesting observation is the presence of the bands at 3014 cm^{-1}, which are related to the release of CH_4, which increases with the temperature, between 400 and 650 °C, reaching its maximum around 500 °C. It is well known that the peaks in the FTIR spectrum at ~3040–2700 cm^{-1} are assigned to a products mixture, which consist of C_3H_8, C_2H_6, C_2H_4 and C_2H_2 whereas the change in absorption intensity are associated with the relative change in concentration of the resulting C—H groups, which could indicate modifications in the pyrolytic cracking mechanism or recombination of gaseous products [30]. This behavior, between 400 and 650 °C, could probably be associated with the end stage of lignin degradation, where one of the major products of the transformation is CH_4.

It is worth noting that at temperature about 100 °C, small amounts of CO_2 was detected, besides water, which suggests that at the beginning of the process, the decarboxylation reaction (formation of CO_2) in the ligno-cellulosic biomass is also favored. However, as the pyrolysis temperature increases, between 180 and 350 °C, the release of H_2O, CO_2 and CO, besides of a mixture organics product, augments significantly, in agreement with the maximums of the weight loss rate, detected at 195 and 312 °C in the DTG curve (see Fig. 4a). The detection of both, CO_2 and CO, in this range of temperature suggests that the decarboxylation (formation of CO_2) and decarboxylation (formation of CO) reactions are simultaneously favored in this stage of the pyrolysis.

Another observation during the qualitative analysis is the presence of a complex mixture of organic compounds, which displayed bands in the regions of 1765–1715, 1505–1560 cm^{-1}, as well as, at 1185 and 1100–1030 cm^{-1}. This region of the spectrum is quite unspecific, because most of the organic compounds have C—H bonds or different oxygen functional groups, such as; C═O, COOH, OH, O—C—O and C—O—C, which, by reformation or cracking eventually decompose into CO_2 and CO [31]. It is also well known that C—H bonds show important absorptions between 1480 and 1450 cm^{-1}, which would indicate the presence of hydrocarbons with two carbon atoms or more, or other moieties of other chemical functionalities [27].

On the other hand, the bands at 1100–1030 cm^{-1} are attributed to alcohols C—O—H bond involving a saturated carbon, formed during the cracking pyrolytic process, so it is not related to the carboxyl groups. Meanwhile the peaks found in the range of 1650–1800 cm^{-1} are assigned to C═O stretching vibrations of the carboxylic acid and/or carbonyl compounds, corresponding to aldehydes, ketones and esters. In addition, the absorption bands at 1240 and 1185 cm^{-1} are assigned to C—O stretching vibration, corresponding to phenolic oxygen [32].

Finally, the bands in the range of 1620–1590 cm^{-1} are attributed to C═C group of unsaturated aromatic compounds, which could be related essentially to the lignin degradation. Lignin is an amorphous cross-linked resin without specific structure and the analysis from their intermediate components is especially difficult due to

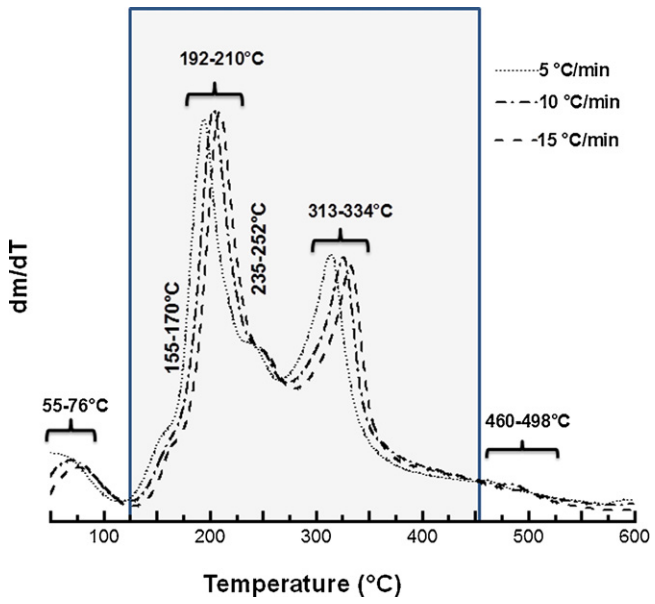

Fig. 5. Effect of heating rate on the DTG curves.

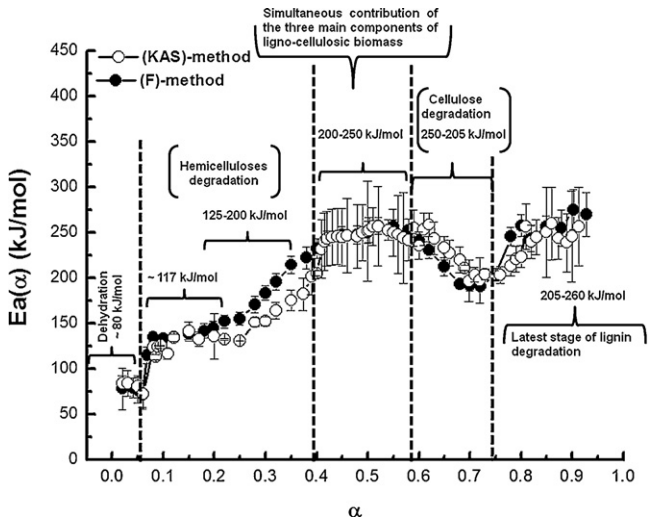

Fig. 6. Apparent activation energy $E_a(\alpha)$ as a function of the extent of reaction α, determined by the Friedman (*F*) and Kissinger–Akahira–Sunose (KAS) methods during thermal pyrolysis of the orange waste, between 50 and 420 °C. *Note*: An experimental error below 10% is also considered (error bars).

the formation of different organic complexes, aromatic hydrocarbons, phenolic, hydrophenolic or aliphatic and methoxy groups, which could be the main products [33]. Furthermore, it should be noted that the C=C stretching band is unique for olefins while the C—H stretching bands, in the range of 3000–2850 cm^{-1}, are caused by both olefins and paraffins [34]. Therefore, the presence of absorptions bands attributed to C=C in the region of 1580 cm^{-1}, would be associated with the degree of insaturation (including aromaticity) of the products.

4.5. Kinetic analysis

The thermal profiles of the decomposition of orange waste at different heating rates (5, 10 and 15 °C min^{-1}) in dynamic nitrogen atmosphere are shown in Fig. 5. For the sake of clarity, the TG curves are presented in their derivative form DTG (dm/dT vs T). In all cases it was observed that an increase in the heating rate only shifts the DTG curves and peak temperature to higher values, without changes in the thermal profile (see Fig. 5). From the kinetics point of view, that thermal behavior suggests that the reaction rate is only function of the temperature and that the pyrolytic cracking mechanism of the reaction is independent of the heating rates, at least under the experimental conditions used in this study.

In order to simplify the analysis through DTG curves (Fig. 5) three large stages during the degradation process were defined: dehydration process for temperatures lower than 120 °C, pyrolytic cracking, from 125 to 450 °C, stage composed by simultaneous and complex process, where the main components, hemicellulose, cellulose and lignin are degraded and a maximum release of volatile matter occur, and, finally, the secondary or last degradation of the lignin, at temperatures above 450 °C. In general, the thermal degradation of orange waste can be depicted according to Scheme 1.

Analysis in terms of activation energy shows the complex $E_a(\alpha)$ on α dependence (Fig. 6), and revealed the typical behavior of complex reactions, involving multiple, parallel and consecutives process during the degradation of biomassic waste in nitrogen atmosphere [35–38]. Fig. 6 shows only the values in the $0.02 \leq \alpha \leq 0.92$ range, corresponding to the temperatures between 50 and 420 °C, because to the results for $\alpha < 0.02$ and $\alpha > 0.92$ are not accurate enough.

It should be noted the excellent agreement between results obtained by both models-free kinetics algorithms, with deviations lower than 10% between the differential Friedman (*F*) and integral Kissinger–Akahira–Sunose (KAS) methods. This agreement validates not only the above-proposed hypothesis but also the reliability of the performed calculations and confirmed the excellent predictive power of the direct methods.

The first stage, related to the orange waste dehydration process, between room temperature and ~120 °C, at $\alpha < 0.1$, shows that the activation energy is independent of the extent of reaction α, with a value ~80 kJ/mol. It should be noted that the $E_a(\alpha)$ values obtained by the application of both methods, are 2–3 times the energy barrier for water diffusion necessary to overcome the van der Waals interactions or the average energy involved in the typical hydrogen

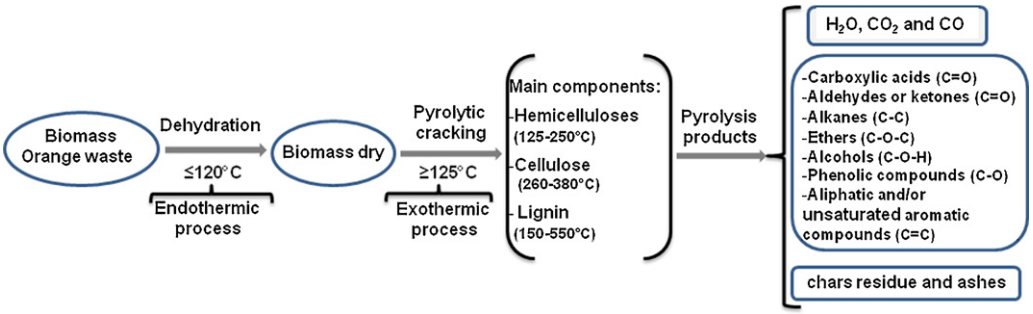

Scheme 1. Stages in ligno-cellulosic orange waste pyrolysis.

bonding [39,40]. That result suggests that the dehydration stage is kinetically controlled by an energy barrier that comprises multiple processes; i.e., breaking hydrogen bonds, water evaporation or water diffusion among others [41]. However, the values of $E_a(\alpha)$ during the dehydration process are in agreement with others values reported for similar processes [37,42].

The dependence of $E_a(\alpha)$ on α associated essentially with hemicelluloses degradation beside simultaneous degradation of lignin hindered by the decomposition of hemicelluloses for temperatures between 125 and 250 °C, shows that initially the activation energy is essentially independent of the degree of transformation (α), with values about 117 kJ/mol, as α changes from 0.1 to 0.25. That behavior suggests that the step that always limits the speed of the reaction is unique and that the pyrolytic breaking reaction occur on well-defined sites. The justification for this behavior it might be related to the lineal polymeric structure of the hemicelluloses. If so, thermal degradation can start rather easily on the weakly link sites inherent to the polymeric lineal chain. Then initial step, related to lower and constant values of activation energy are most likely associated with the initiation of the process that occurs at these weak links. By contrast, during the second step of degradation, as α change from 0.25 to 0.4, an increase in the $E_a(\alpha)$ values is observed, as the reaction proceeds, revealing a typical behavior between competitive reactions [43,44]. Once the weaker bonds are broken, the limiting step of degradation shifts toward to degradation by random scissions of lineal chain, which typically promote an increase in the activation energy [45,46]. Therefore, the existence of this zone, with slope changes at $\alpha = 0.25$, is a clear indication that reveals a change of mechanism of the pyrolytic breaking bonds and suggest that the energetic barrier necessary to overcome different interactions during the last step of hemicelluloses pyrolysis degradation, comprises multiple and simultaneous processes [47–49]. This behavior may be attributed to the cross-linked nature of the residual solid, composed essentially by cellulose and lignin, besides residual products of the hemicelluloses degradation, where the main problems will be associated to heat- and mass-transfer processes.

As it can be observed the contiguous stage, between $0.4 \leq \alpha \leq 0.60$, shows a progressive increasing in the $E_a(\alpha)$ values, from ~200 kJ/mol corresponding to the end step of hemicelluloses degradation, up to reach an average of 250 kJ/mol. Curiously, during this stage both the evolved energy (see DSC curves, Fig. 2) and gaseous products (see FTIR results, Fig. 4b) reach a maximum. However, the DTG curve of biomass degradation show a wide and very slow weight losses, with a gently sloping baseline that makes difficult to define a particular behavior or assignation. The justification for this behavior on this intermediate stage it might be related to the simultaneous contribution of the three main components of lignocellulosic biomass (hemicelluloses, cellulose and lignin) [8]. In this sense, the result indicates the competitive character of the processes during that stage and that the activation energy behavior is likely associated with the process of cross-linked polymer degradation. Therefore, these results denote that degradation mechanism correspond to the breakage of weak bonds inside of a cross-linked polymer matrix and diffusion of gaseous species.

The $E_a(\alpha)$ curve from 270 to 350 °C, show that the values of $E_a(\alpha)$ decreases from about 250 kJ/mol at $\alpha = 0.60$, until an average of 205 kJ/mol for $\alpha = 0.70$. This dependence of $E_a(\alpha)$ on α is typical of a multiple-steps reaction initially limited by a diffusion mechanism [45,47]. Similarly, the pyrolysis degradation of cellulose in the matrix could also be affected by the presence or simultaneous degradation of lignin and residues from the hemicelluloses degradation. The initial decrease may be caused by the diffusional limitations of the released gaseous species, generated before and during the pyrolytic cracking, leading to continuous changes in the solid residual composition. Afterwards, the $E_a(\alpha)$ values reach a minimum and the activation energy is essentially constant, ~205 kJ/mol, as α changes from 0.70 to 0.78. Again, this behavior indicates that the degradation mechanism has unique characteristics and that the pyrolysis degradation of cellulose occurs on functional groups energetically equivalents, inside of the polymeric matrix. These considerations suggest that the degradation of cellulose starts on the weak bonds of the functional groups in the polymeric network and that pyrolytic decomposition in an inert atmosphere occurs in such a way that they tend to preserve the structure, thus bond breaking inside the polymer requires a large amount of energy.

Finally, an increase of $E_a(\alpha)$ on α values up to a maximum value of approximately 260 kJ/mol for $\alpha < 0.92$, near the end of the reaction was observed. That interval was attributed to the last stage degradation of lignin. The decomposition of the polymeric structure in the lignin starts at relatively low temperatures, about of 150–200 °C, and the main process occurs around 400 °C, with the formation of aromatic hydrocarbons, phenolics, hydrophenolics and guaiacyl/syringyl-type compounds, besides products having phenolic —OH groups [48,49]. The analysis during this step is especially difficult because complex phenolic species from lignin decomposition leads to CO_2 release from the carboxyl groups, H_2O from the hydroxyl groups, CO from the weakly bound oxygen groups, such as aldehyde groups, and H_2 from the aliphatic and methoxy groups. The situation is especially complicated, by the fact that the gaseous products and the inhomogeneities in the network structure are strongly influenced by the reaction temperature, heating rate and degradation atmosphere. All these difficulties, besides of the high amount of residual matter until this point, are probably responsible for the particular shape of the activation energy profile during the last stage of process and reveals the typical behavior between competitive reactions, comprising of multiple and simultaneous processes.

In general, the observed activation energy values in the 120–250 kJ/mol range from are similar to those reported by other authors for the pyrolysis degradation of ligno-cellulosic biomass [25,28,50,51]. However, it should be noted that to our best knowledge, this is the first report that described a systematic and detailed thermo-kinetics study of each stage, together with gaseous products, during the pyrolytic process of a raw material ligno-cellulosic derivative from orange waste.

5. Conclusions

The thermal behavior of the orange waste decomposition can be interpreted as a multiple and simultaneous processes, due to its complex composition and structure, which difficult their assignation and interpretation.

Simultaneous TGA–FTIR analysis revealed that the volatile compounds evolved between 50 and 600 °C are mainly: H_2O, CO_2 and CO, besides of a mixture of organic products composed by carboxylic acids, aldehydes or ketones (C═O), alkanes (C—C), ethers (C—O—C), alcohols (C—O—H), phenolic compounds (C—O) and aliphatic and/or unsaturated aromatic compounds (C═C).

The results according to the model-free-kinetics algorithms used in this study shows the complex $E_a(\alpha)$ on α dependence and revealed that the main processes during the degradation of biomassic waste in nitrogen atmosphere can be summarized as:

- Dehydration process, between room temperature and ~120 °C, at $\alpha < 0.1$ with activation energy values $E_a(\alpha) \approx 80$ kJ/mol.
- Hemicelluloses degradation, between 125 and 250 °C, process that takes place in two consecutive stages: (i) pyrolytic breaking on well-defined sites, where the $E_a(\alpha)$ values ~117 kJ/mol, are independent of the degree of transformation (α), for α between 0.1 and 0.25; and (ii) as α change from 0.25 to 0.4, where

activation energy values increase up to 200 kJ/mol, revealing a typical behavior between competitive reactions.

- An intermediate interval, between $0.4 \leq \alpha \leq 0.60$, characterized by a wide and very slow weight losses, shows a increases in the $E_a(\alpha)$ values from about 200 kJ/mol up to 250 kJ/mol related to the simultaneous contribution of the three main components in the ligno-cellulosic biomass.
- Cellulose degradation, between 260 and 380 °C, where the values of $E_a(\alpha)$ decreases from 250 kJ/mol at $\alpha = 0.60$, until 205 kJ/mol for $\alpha = 0.70$, describing the typical behavior of a multi-step reaction, initially controlled by diffusion. As α changes from 0.70 to 0.78 and $E_a(\alpha)$ values reach a minimum ~205 kJ/mol, the degradation mechanism is unique and the degradation occurs on functional groups energetically equivalents, inside of polymeric matrix.
- Finally, during the last stage, the increase of $E_a(\alpha)$ on α values up to ~260 kJ/mol for $\alpha < 0.92$, is attributed to the last stage degradation of lignin and the particular shape of the activation energy profile can be related to the inhomogeneities in the network structure and high amount of residual solid.

References

[1] G. van Rossum, S.R.A. Kerten, W.P.M. van Swaaij, Catalytic and noncatalytic gasification of pyrolysis oil, Industrial and Engineering Chemistry Research 46 (2007) 3959–3967.
[2] A.V. Bridgwater, Principles and practice of biomass fast pyrolysis processes for liquids, Journal of Analytical and Applied Pyrolysis 51 (1999) 3–22.
[3] V. Ferreira-Leitao, L.M. Fortes Gottschalk, M.A. Ferrara, A. Lima Nepomuceno, H.B. Correa Molinari, E.P.S. Bon, Biomass residues in Brazil: availability and potential uses, Waste and Biomass Valorization 1 (2010) 65–76.
[4] FAOSTAT, Food and Agricultural commodities production, Statistical Database (2010), consulted in July 2012. http://faostat.fao.org/site/339/default.aspx
[5] E. Ranzi, A. Cuoci, T. Faravelli, A. Frassoldate, G. Migliavacca, S. Pierucci, S. Sommariva, Chemical kinetics of biomass pyrolysis, Energy and Fuels 22 (2008) 4292–4300.
[6] A.V. Bridgwater, G.V.C. Peacocke, Fast pyrolysis process for biomass, Renewable and Sustainable Energy Reviews 4 (2000) 1–73.
[7] K.S. Shanmukharadhya, Simulation and thermal analysis of the effect of fuel size on combustion in an industrial biomass furnace, Energy and Fuels 21 (2007) 1895–1900.
[8] H. Yang, R. Yan, H. Chen, C. Zheng, D.H. Lee, D.T. Liang, In-depth investigation of biomass pyrolysis based on three major components: hemicellulose, cellulose and lignin, Energy and Fuels 20 (2006) 388–393.
[9] B. Zapata, J. Balmaseda, E. Fregoso-Israel, E. Torres-Garcıa, Thermo-kinetics study of orange peel in air, Journal of Thermal Analysis and Calorimetry 98 (2009) 309–315.
[10] J. Manganaro, B. Chen, J. Adeosun, S. Lakhapatri, D. Favetta, A. Lawal, Conversion of residual biomass into liquid transportation fuel: an energy analysis, Energy and Fuels 25 (2011) 2711–2720.
[11] D. Mohan, C.U. Pittman Jr., P.H. Steele, Pyrolysis of wood/biomass for bio-oil: a critical review, Energy and Fuels 20 (2006) 848–889.
[12] C.J. Mulligan, L. Strezov, V. Strezov, Thermal decomposition of wheat straw and mallee residue under pyrolysis conditions, Energy and Fuels 24 (2010) 46–52.
[13] M. Stenseng, A. Jensen, K. Dam-Johansen, in: A.V. Bridgwater (Ed.), Progress in Thermochemical Biomass Conversion, Blackwell Science, Oxford, UK, 2001, pp. 1061–1075.
[14] R. Miranda, D. Bustos-Martinez, C. Sosa Blanco, M.H. Gutierrez Villarreal, M.E. Rodriguez Cantu, Pyrolysis of sweet orange (Citrus sinensis) dry peel, Journal of Analytical and Applied Pyrolysis 86 (2009) 245–325.
[15] L. Aguiar, F. Márquez-Montesinos, A. Gonzalo, J.L. Sánchez, J. Arauzo, Influence of temperature and particle size on the fixed bed pyrolysis of orange peel residues, Journal of Analytical and Applied Pyrolysis 83 (2008) 124–130.
[16] S. Vyazovkin, A.K. Burnham, J.M. Criado, L.A. Perez-Maqueda, C. Popescu, N. Sbirrazzuoli, ICTAC Kinetics Committee recommendations for performing kinetic computations on thermal analysis data, Thermochimica Acta 520 (2011) 1–19.
[17] S. Vyazovkin, Modification of the integral isoconversional method to account for variation in the activation energy, Journal of Computational Chemistry 22 (2001) 178–183.
[18] H.L. Friedman, Kinetics of thermal degradation of char-forming plastics from thermogravimetry. Application to a phenolic plastic, Journal of Polymer Science Part C 6 (1963) 183–195.
[19] T. Akahira, T. Sunose, Method of determining activation deterioration constant of electrical insulating materials, Report of Research Institute. Chiba Institute of Technology (Science Technology) 16 (1971) 22–31.
[20] H.E. Kissinger, Reaction kinetics in differential thermal analysis, Analytical Chemistry 29 (1957) 1702–1706.
[21] A.W. Coats, J.P. Redfern, Kinetic parameters from thermogravimetric data, Nature 201 (1964) 68–69.
[22] H. Yang, R. Yan, H. Chen, H.D. Lee, C. Zheng, Characteristics of hemicellulose, cellulose and lignin pyrolysis, Fuel 86 (2007) 1781–1788.
[23] P. Mckendry, Energy production from biomass (part 1): overview of biomass, Bioresource Technology 83 (1) (2002) 37–46.
[24] A. Demirbas, Mechanisms of liquefaction and pyrolysis reactions of biomass, Energy Conversion and Management 41 (6) (2000) 633–646.
[25] M. Amutio, G. Lopez, R. Aguado, M. Artetxe, J. Bilbao, M. Olazar, Kinetic study of lignocellulosic biomass oxidative pyrolysis, Fuel 95 (2012) 305–311.
[26] E. Ranzi, A. Cuoci, T. Faravelli, A. Frassoldati, G. Migliavacca, S. Pierucci, S. Sommariva, Chemical kinetics of biomass pyrolysis, Energy and Fuels 22 (2008) 4292–4300.
[27] G. Hu, C. Cateto, Y. Pu, R. Samuel, A.J. Ragauskas, Structural characterization of switchgrass lignin after ethanol organosolv pretreatment, Energy and Fuels 26 (2012) 740–745.
[28] J.J.M. Orfao, F.J.A. Antunes, J.L. Figueiredo, Pyrolysis kinetics of lignocellulosic materials-three independent reactions model, Fuel 78 (1999) 349–358.
[29] Ch.J. Pouchert (Ed.), The Aldrich Library of FT-IR Spectra Vapor Phase, 1st Ed.; Aldrich Chemical Company, Inc.: Milwaukee, Wisconsin, U. S. A., 1989; Vol. 3, Chapter. Non-Aromatic Alcohols, pp. 155–263 and Chapter. Non-Aromatic anhydrides, pp. 759–63.
[30] S.A. Nair, T. Nozaki, K. Okazaki, In situ Fourier transform infrared (FTIR) study of nonthermal-plasma-assisted methane oxidative conversion, Industrial and Engineering Chemistry Research 46 (11) (2007) 3486–3496.
[31] S.B. Souza, A.P.D. Moreira, A.M.R.F. Teixeira, TG–FTIR coupling to monitor the pyrolysis products from agricultural residues, Journal of Thermal Analysis and Calorimetry 97 (2009) 637–642.
[32] M. Mohan, N.K. Gupta, M. Kumar, Synthesis, magnetic and electrochemical properties of binuclear copper(II) complexes of pyridoxal hydrazones, Inorganica Chimica Acta 197 (1992) 39–46.
[33] M.P. Pandey, C.S. Kim, Lignin depolymerization and conversion: a review of thermochemical methods, Chemical Engineering and Technology 34 (2011) 29–41.
[34] I.U. Mohsin, D. Lager, C. Gierl, W. Hohenauer, H. Danninger, Thermo-kinetics study of MIM thermal de-binding using TGA coupled with FTIR and mass spectrometry, Thermochimica Acta 503–504 (2010) 40–45.
[35] D. Cancellier, V. Leroy-Cancellieri, E. Leoni, A. Simeoni, A.Ya. Kizin, A.I. Filkov, G. Rein, Kinetic investigation on the smouldering combustion of boreal peat, Fuel 93 (2012) 479–485.
[36] J. Wang, M.P.G. Laborie, M.P. Wolcott, Comparison of model-free kinetic methods for modeling the cure kinetics of commercial phenol-formaldehyde resins, Thermochimica Acta 439 (2005) 68–73.
[37] E. Torres-Garcia, J. Balmaseda, L.F. del Castillo, E. Reguera, Thermal evolution of microporous nitroprussides on their dehydration process, Journal of Thermal Analysis and Calorimetry 86 (2) (2006) 371–377.
[38] G. Rodriguez-Gattorno, L.F. del Castillo, E. Torres-Garcia, Combined use of high resolution TGA with the isoconversion method: kinetic analysis of the thermal dehydration of $KNbWO_6 \cdot H_2O$, Thermochimica Acta 435 (2005) 176–180.
[39] W. Feyereisen Martin, D. Feller, D.A. Dixon, Hydrogen bond energy of the water dimer, Journal of Physical Chemistry 100 (8) (1996) 2993–2997.
[40] T. Steiner, The hydrogen bond in the solid state, Angewandte Chemie International Edition 41 (1) (2002) 48–76.
[41] J.S. Valente, G. Rodriguez-Gattorno, M. Valle-Orta, E. Torres-Garcia, Thermal decomposition kinetics of MgAl layered double hydroxides, Materials Chemistry and Physics 133 (2012) 621–629.
[42] A.K. Galwey, Structure and order in thermal dehydrations of crystalline solids, Thermochimica Acta 355 (2000) 181–238.
[43] S.V. Vyazovkin, A.I. Lesnikovich, An approach to the solution of the inverse kinetic problem in the case of complex processes: part 1. Methods employing a series of thermoanalytical curves, Thermochimica Acta 165 (1990) 273–280.
[44] G. He, B. Riedl, A. Aït-Kadi, Model-free kinetics: curing behavior of phenol formaldehyde resins by differential scanning calorimetry, Journal of Applied Polymer Science 87 (2003) 433–440.
[45] J.D. Peterson, S. Vyazovkin, C.A. Wight, Kinetics of the thermal and thermo-oxidative degradation of polystyrene, polyethylene and poly(propylene), Macromolecular Chemistry and Physics 202 (2001) 775–784.
[46] A. Valor, S. Kycia, E. Torres-Garcia, E. Reguera, C. Vazquez-Ramos, F. Sanchez-Sinencio, Structural and thermal study of calcium undecanoate, Journal of Solid State Chemistry 172 (2003) 471–479.
[47] E. Torres-García, A. Peláiz Barranco, C. Vázquez, F. Calderón Piñar, O. Pérez Martínez, Oxidation kinetic study of copper(I) in ferroelectric ceramic $[PbTiO_3–PbZrO_3–PbCuNbO_3 + 0.5\ mol\%MnO_2]$ system by high resolution thermogravimetric analysis, Thermochimica Acta 372 (2001) 39–44.
[48] J. Rodriguez, J. Graca, H. Pereira, Influence of tree eccentric growth on syringyl/guaiacyl ratio in *Eucalyptus globulus* wood lignin assessed by analytical pyrolysis, Journal of Analytical and Applied Pyrolysis 481 (2001) 58–59.
[49] R. Alén, E. Kuoppala, P. Oesch, Formation of the main degradation compound groups from wood and its components during pyrolysis, Journal of Analytical and Applied Pyrolysis 36 (1996) 137–148.
[50] G. Várhegyi, B. Bobály, E. Jakab, H. Chen, Thermogravimetric study of biomass pyrolysis kinetics. A distributed activation energy model with prediction tests, Energy and Fuels 25 (2011) 24–32.
[51] R. Mehrabian, R. Scharler, I. Obernberger, Effects of pyrolysis conditions on the heating rate in biomass particles and applicability of TGA kinetic parameters in particle thermal conversion modeling, Fuel 93 (2012) 567–575.